

Supporting Information

Large stokes shift NIR fluorescent probe for visual monitoring of mitochondrial peroxynitrite during inflammation and ferroptosis and in Alzheimer's disease model

Shiyong Chen^a, Wei Huang^a, Hongli Tan^a, Guoxing Yin^a, Shengyou Chen^a, Kuicheng Zhao^a,

Yinghui Huang^a, Youyu Zhang, Haitao Li and Cuiyan Wu^{*a,b}

^aCollege of Chemistry and Chemical Engineering, Hunan Normal University,
Changsha 410081, PR China

^bSchool of Materials and Chemical Engineering, Ningbo University of Technology, Ningbo
315211, PR China

* Corresponding author: Tel: +86-731-88865515; Fax: +86-731-88865515;

E-mail: Cuiyan-wu@nbut.edu.cn

*Corresponding author: +86-731-88865515; Fax: +86-731-88865515;

E-mail address: Cuiyan Wu (Cuiyan-wu@nbut.edu.cn),

1. Preparation of Various Analytes

Preparation of HClO: After diluting commercial sodium hypochlorite solution, the absorbance value at 292 nm was measured by UV-VIS absorption spectrum, and the concentration of hypochlorite was calculated according to Lambert-Beer's law ($\epsilon=350 \text{ M}^{-1} \text{ cm}^{-1}$).

Preparation of H₂O₂: Commercial hydrogen peroxide solution (30%) was diluted, the absorbance value at 240 nm was measured by UV-VIS absorption spectrum, and the concentration of hydrogen peroxide was calculated according to the Lambert-Beer law ($\epsilon=43.6 \text{ M}^{-1} \text{ cm}^{-1}$).

Preparation of HO•: Hydroxyl radical solution (50 mM) was prepared by adding aqueous ferrous sulfate (50 mM) to aqueous hydrogen peroxide (500 mM) according to the Fenton reaction.

Preparation of O₂^{•-}: 100 mM solution of superoxide anion could be prepared by dissolving 70 mg of potassium superoxide in 10 mL of DMSO.

Preparation of ¹O₂: ¹O₂ solution (50 mM) could be prepared by rapidly adding 50 mM aqueous hypochlorous acid to 100 mM aqueous hydrogen peroxide.

Preparation of NO: Sodium nitroferricyanide (149 mg) was dissolved in 10 mL of deionized water to prepare a 50 mM NO solution.

Preparation of TBHP: 64 mg of a 70% solution of TBHP was diluted to 10 mL with deionized water to make a 50 mM TBHP solution.

Preparation of ONOO⁻: A mixed solution of sodium nitrite (0.6 M) and hydrogen peroxide (0.7 M) was acidified with hydrochloric acid solution (0.6 M) at 0 °C. Then NaOH (1.5 M) was added rapidly (~1-2 s) within 1-2 s to make the solution alkaline. The solution was passed through a short MnO₂ column to remove excess H₂O₂. The concentration of the as-prepared ONOO⁻ was calibrated by measuring its absorbance at 302 nm ($\epsilon=1670 \text{ M}^{-1} \cdot \text{cm}^{-1}$) by UV-VIS absorption spectroscopy.

2. Measurement methods

Calculation of fluorescence quantum yield

The spectra of fluorescence quantum yield were obtained using 1-cm quartz cuvettes and spectroscopic grade solvents. Based on the absorption of the test sample, rhodamine B in ethanol was employed as the fluorescence quantum yield calculation standard ($\phi_{stand} = 0.97$). To reduce reabsorption effects, the absorbance of the samples was kept below 0.05. The following equation was used to calculate the quantum yields:

$$\phi_{s\text{amp}} = \phi_{s\text{tand}} \left(\frac{n_{s\text{amp}}}{n_{s\text{tand}}} \right)^2 \left(\frac{A_{s\text{tand}}}{A_{s\text{amp}}} \right) \left(\frac{F_{s\text{amp}}}{F_{s\text{tand}}} \right)$$

F denotes the integral of the corrected fluorescence spectrum; A is the absorbance at the excitation wavelength; n is the refractive index of the solvent.

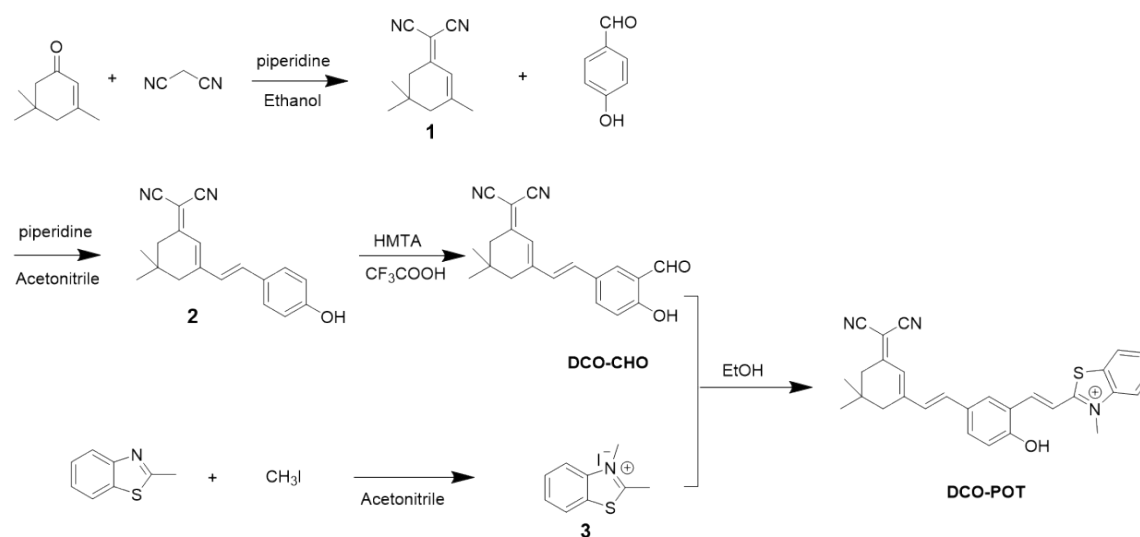
Calculation of detection limit

The detection limit was determined using the fluorescence titration. The fluorescence emission spectra of probe DCO-POT were measured 10 times to establish the standard deviation of the blank measurement. To gain the slope, the fluorescence intensity (670 nm) was plotted as the increasing concentrations of ONOO^- . The detection limit was determined using the following equation:

$$LOD = 3\sigma/k$$

where σ is the standard deviation of blank measurements and k is the slope between fluorescence intensity and ONOO^- concentration.

3. Synthesis and Characterization



Scheme S1. The synthetic route of DCO-POT.

Compound 1 and Compound 2: according to a published literature[1], Weigh isophorone (ISO, 2 g, 10.74 mmol) and malononitrile (1.44 g, 11.82 mmol) into a 100 mL round-bottomed flask, then add 50 mL of absolute ethanol and 1 mL of piperidine, and the reaction solution was refluxed for 12 h. The solvent ethanol was distilled off under reduced pressure, and the crude product was subjected to silica gel column chromatography (PE/DCM=50:1) to obtain a white solid 1 (2 g, yield 92%), (3,5,5-trimethylcyclohexyl-2 - alkylidene) malononitrile. Compound 1 (1.86 g, 10.0 mmol)

and p-hydroxybenzaldehyde (1.22 g, 10.0 mmol) were dissolved in 25.0 mL of acetonitrile solution, a catalytic amount of piperidine was added dropwise to the reaction system, and the mixture was refluxed at 80 °C overnight. After removing the solvent under reduced pressure, the crude product was separated and purified by silica gel column chromatography (eluent: dichloromethane) to obtain orange compound 2 (1.96 g, yield 67.5%).

Compound 3: Synthesized with reference to document [2], methyl iodide (1.77 g, 12.5 mmol) was added to a solution of 2-methylbenzothiazole (0.75 g, 5 mmol) in acetonitrile (15 mL). The mixture was refluxed under N₂ atmosphere for 24 h, and white solid was precipitated. After cooling, suction filtration and washing with cold acetonitrile 3 times gave white compound 3 (1.2 g, yield 89%), which was directly used in the next reaction without further purification.

DCO-CHO: compound 2 (0.5 g, 1.72 mmol) and hexamethyl tetramine (0.25 g, 1.78 mmol) was dissolved in trifluoroacetic acid (15.0 mL) and the reaction was carried out at 90°C for 6-7 hours and passed through TLC monitor. After the reaction was completed, the reaction solution was neutralized to weakly acidic or neutral with sodium hydroxide. Extracted by EA, dried over anhydrous sodium sulfate, the solvent was removed under reduced pressure, and the crude product was purified by column chromatography (eluent: DCM) to obtain a yellow solid DCO-CHO (0.35 g, yield 55%). ¹H NMR (500 MHz, DMSO-*d*₆) δ = 11.18 (s, 1H), 10.28 (s, 1H), 7.96 (d, J = 2.0 Hz, 1H), 7.88 (d, J = 8.7 Hz, 1H), 7.29 (d, J = 2.9 Hz, 1H), 7.03 (d, J = 8.7 Hz, 1H), 6.86 (s, 1H), 6.54 (s, 1H), 2.21 (s, 2H), 2.03 (s, 2H), 1.00 (s, 3H), 0.94 (s, 3H). ¹³C NMR (126 MHz, DMSO-*d*₆) δ=191.04, 170.71, 162.31, 156.53, 137.17, 135.60, 129.15, 128.38, 128.06, 123.07, 122.68, 118.46, 114.42, 113.59, 76.23, 42.70, 38.53, 32.09, 27.89, 26.80.

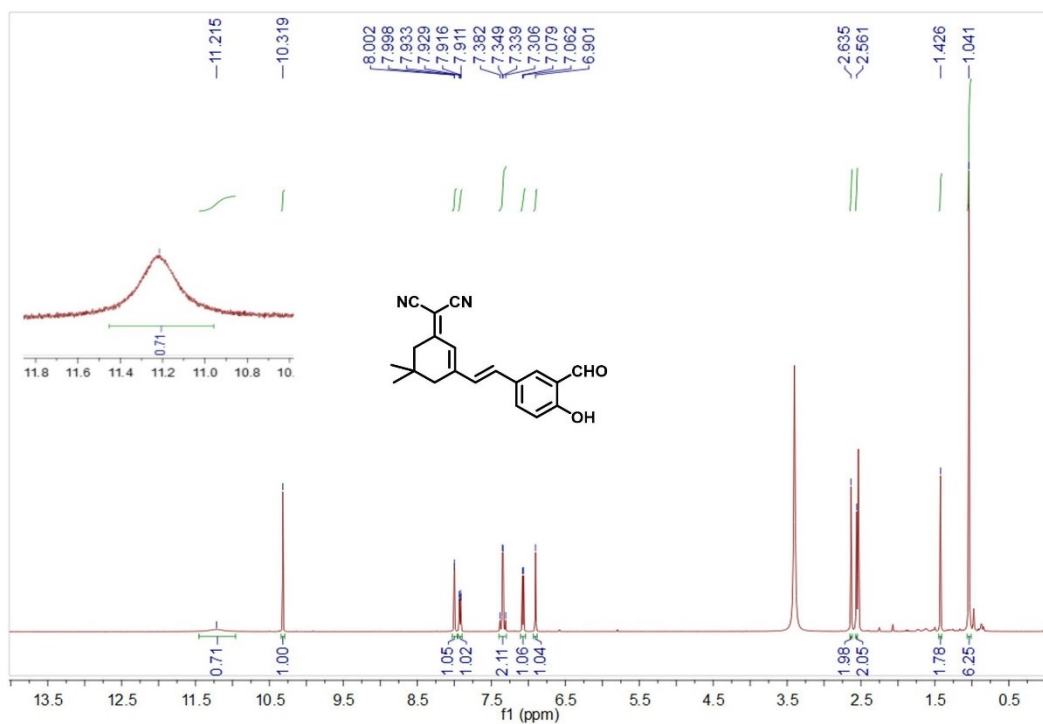


Fig. S1. ^1H NMR spectrum of **DOC-CHO** in $\text{DMSO-}d_6$ (500 MHz).

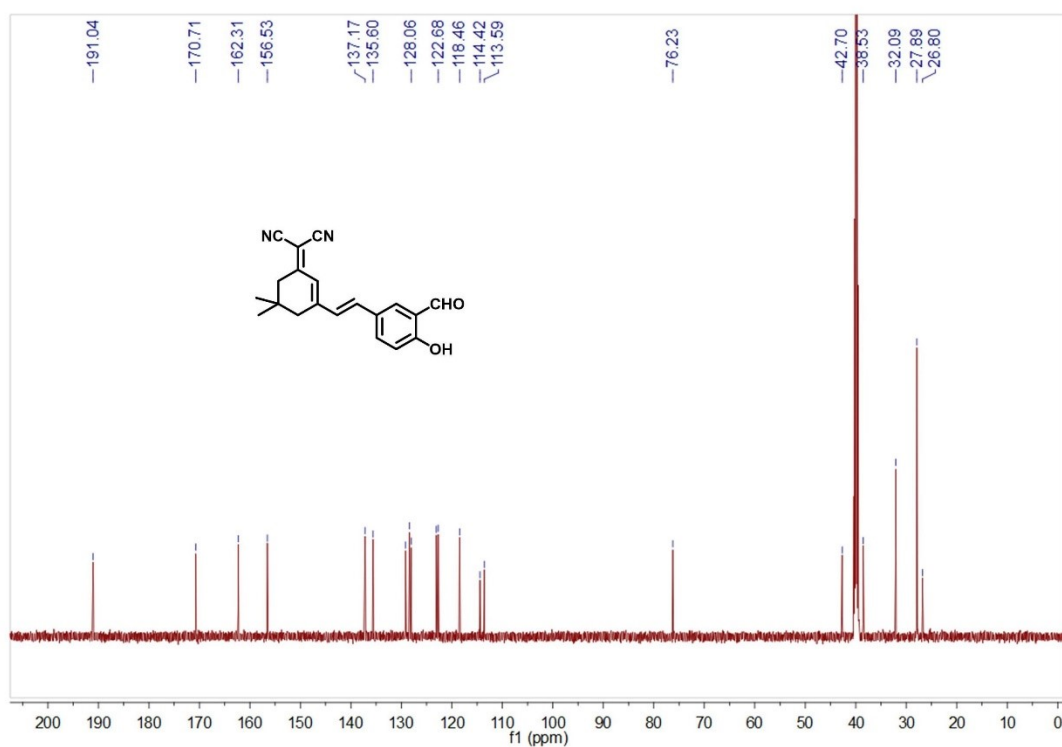


Fig. S2. ^{13}C NMR spectrum of **DOC-CHO** in $\text{DMSO-}d_6$ (126 MHz).

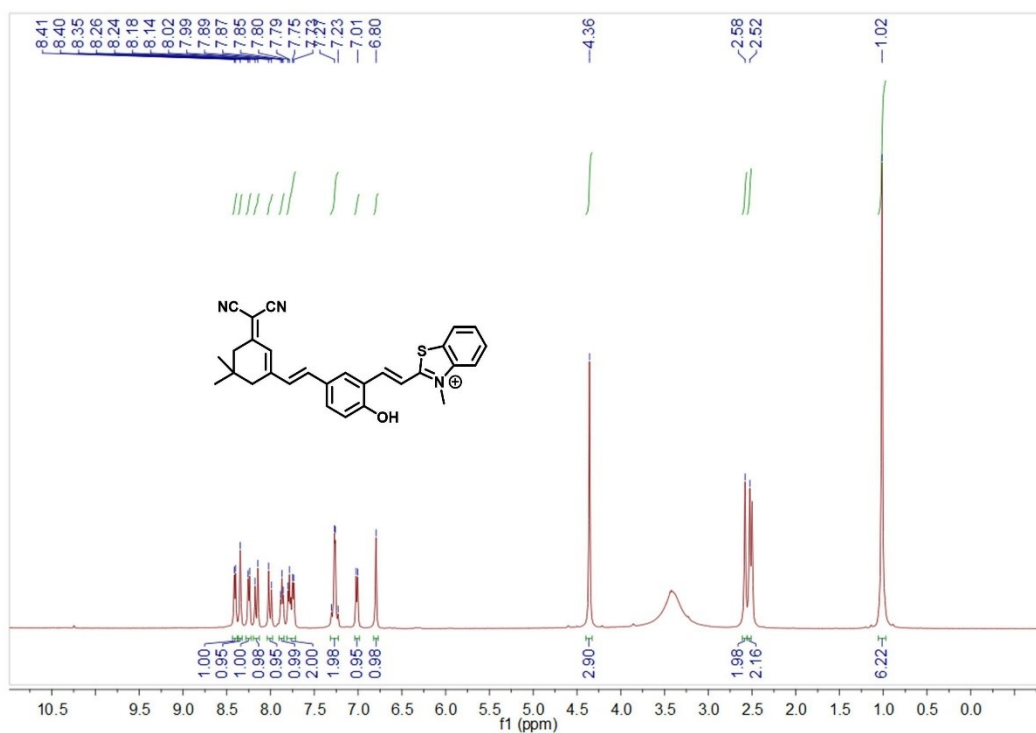


Fig. S3. ^1H NMR spectrum of probe **DOC-POT** in $\text{DMSO-}d_6$ (500 MHz).

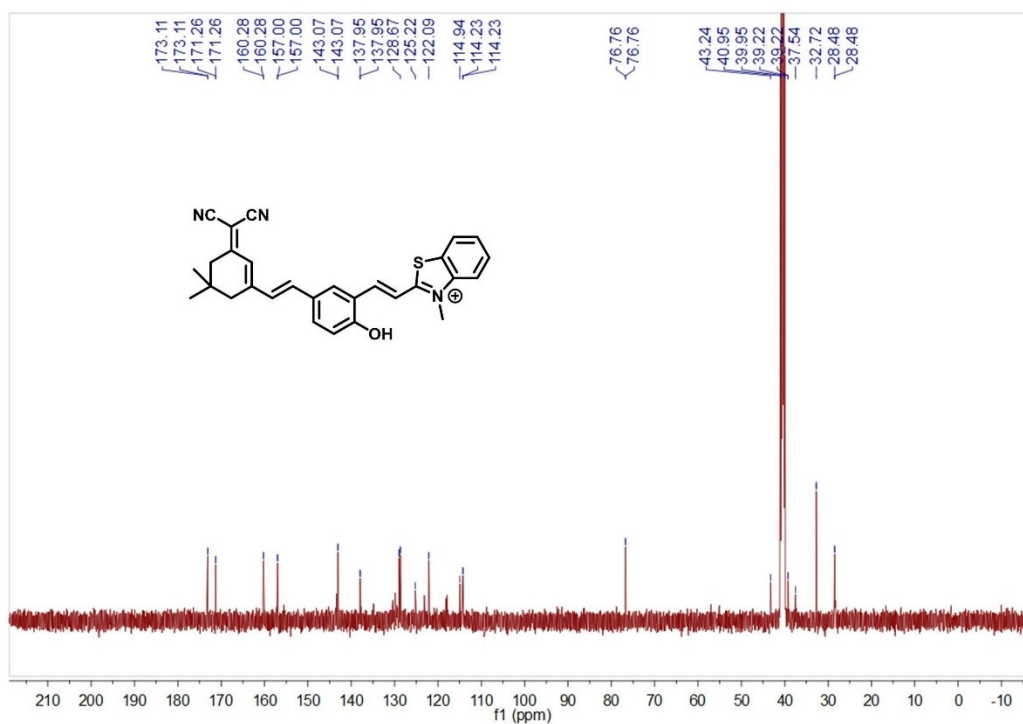


Fig. S4. ^{13}C NMR spectrum of probe **DOC-POT** in $\text{DMSO-}d_6$ (126 MHz).

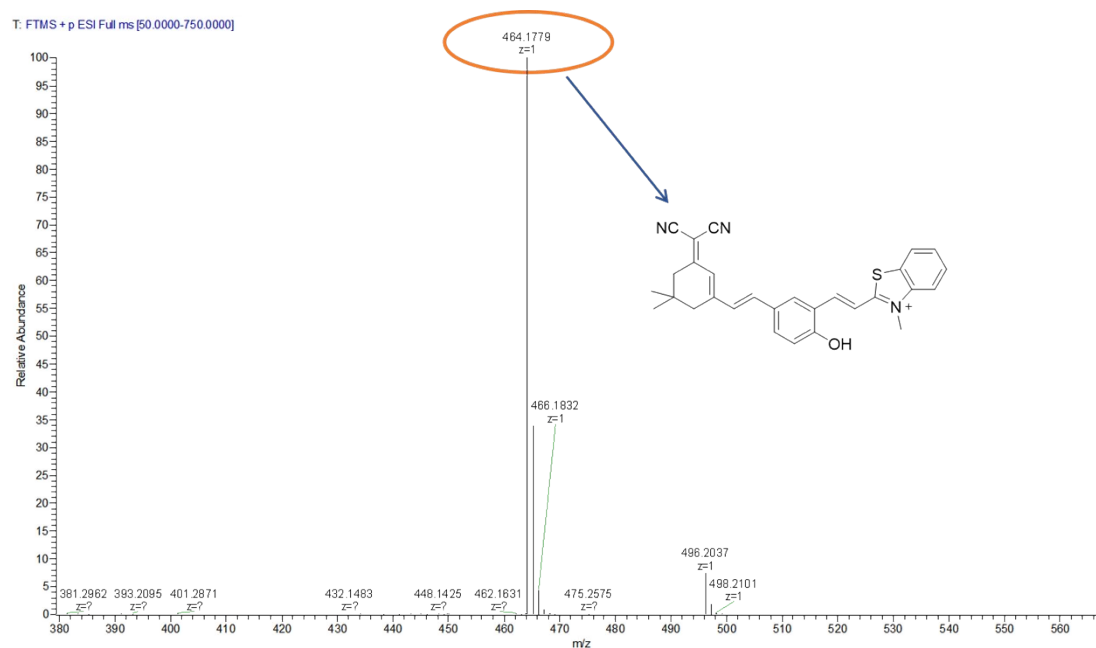


Fig. S5. HRMS spectrum of DCO-POT.

4. Optimization of detection conditions

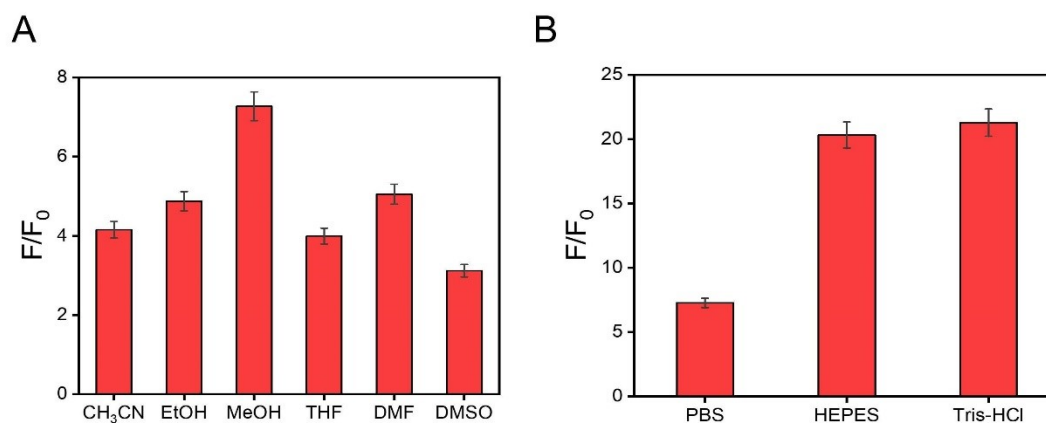


Fig. S6. The effect of different organic solvent (A) and buffer solutions(pH=7.4) (B) on the fluorescence intensity 670 nm of probe DCO-POT (10 μ M) in the presence of ONOO⁻ (20 μ M). ($\lambda_{ex}/\lambda_{em}$ = 500/670 nm, slits: 5 nm/5 nm)

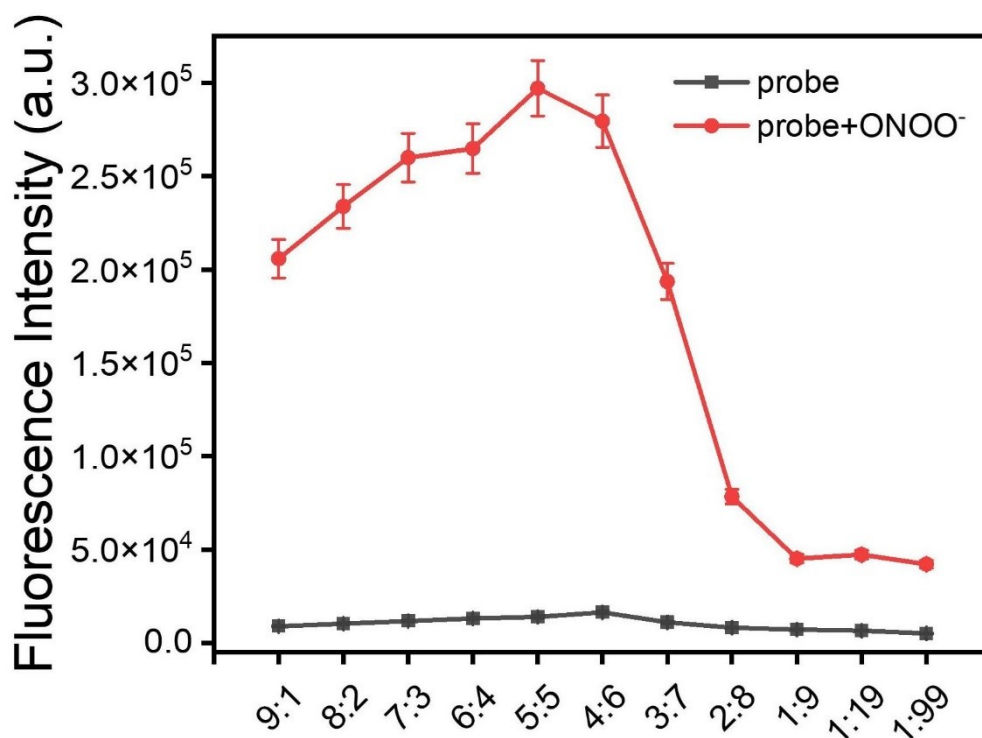


Fig. S7. Fluorescence intensity 670 nm of probe DCO-POT (10 μ M) on addition of ONOO⁻ (20 μ M) in different ratios of MeOH-(Tris-HCl) solution. (pH=7.4, $\lambda_{ex}/\lambda_{em}$ = 500/670 nm, slits: 5 nm/5 nm)

5. Mechanistic investigation

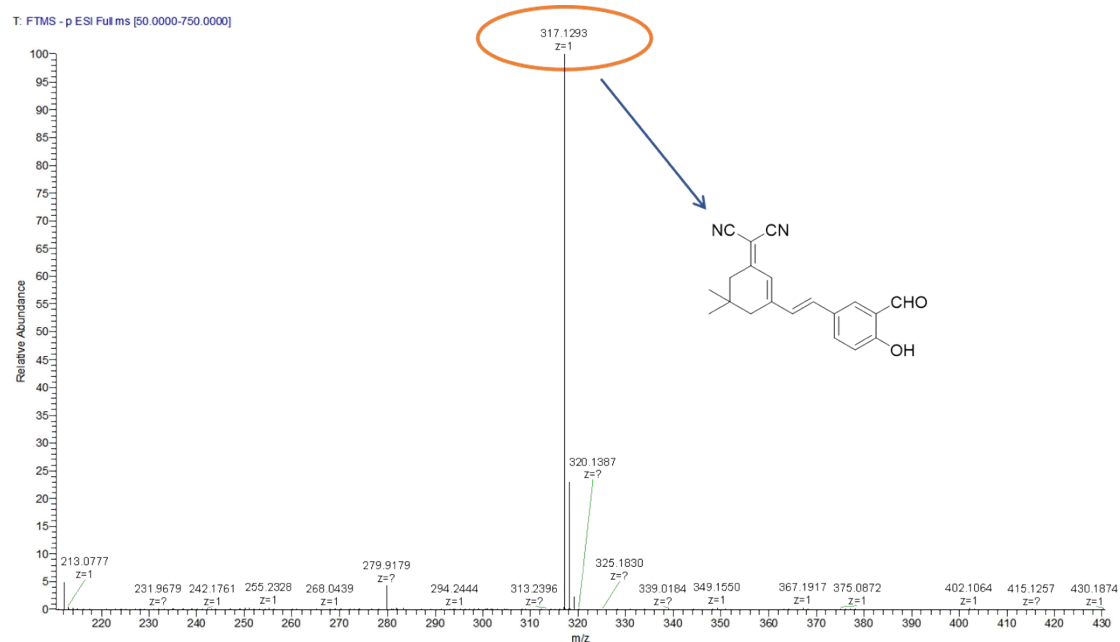


Fig. S8. HRMS spectrum of DCO-POT+ONOO⁻.

6. Colorimetric detection of ONOO⁻ in solution



Fig. S9. (A) Photographs for color changes of DCO-POT chemosensory upon addition of different concentrations of ONOO⁻ under visible light (B) Fluorescence photographs of DCO-POT (10 μM) subjected to different concentrations of ONOO⁻ under 365nm UV light. All photos were taken by iPhone12. (From a to i: adding 0, 2, 4, 6, 8, 10, 12, 15, 20 μM ONOO⁻)

7. Pseudo-first-order rate constant study.

Time-course experiments was determined under the condition of 10 μM probe DCO-POT and 20 μM ONOO⁻ in an MeOH-(Tris-HCl) (1:1 vol%) solution at 25 °C. The fluorescence intensity was recorded at 670 nm with excitation at 500 nm. To estimate the reaction constant of protein labeling, we applied the pseudo-first-order rate law by setting [probe] ≫ [ONOO⁻]. The reaction of the probe DCO-POT (10 μM) with ONOO⁻ (20 nM) in pH 7.4 MeOH-(Tris-HCl) (1:1 vol%) solution was monitored using the fluorescence intensity at 670 nm. The reaction was carried out at 25 °C. The fluorescence data were converted to labeled fractions based on the following equation:

$$[\text{Labeled fraction}] = (F_t - F_0)/(F_{\text{max}} - F_0) \quad (1)$$

where F_t denotes the fluorescence intensity at various periods, F_0 denotes the fluorescence intensity of the probe solution, and F_{max} denotes the maximum fluorescence intensity once the reaction is complete.

The fictitious first-order rate constant is represented by k' . By fitting the fluorescence data using the following equation, it was possible to obtain the pseudo-first-order rate constant, k_{obs} :

$$[\text{Labeled fraction}] = 1 - \exp(-k_{\text{obs}}t) \quad (2)$$

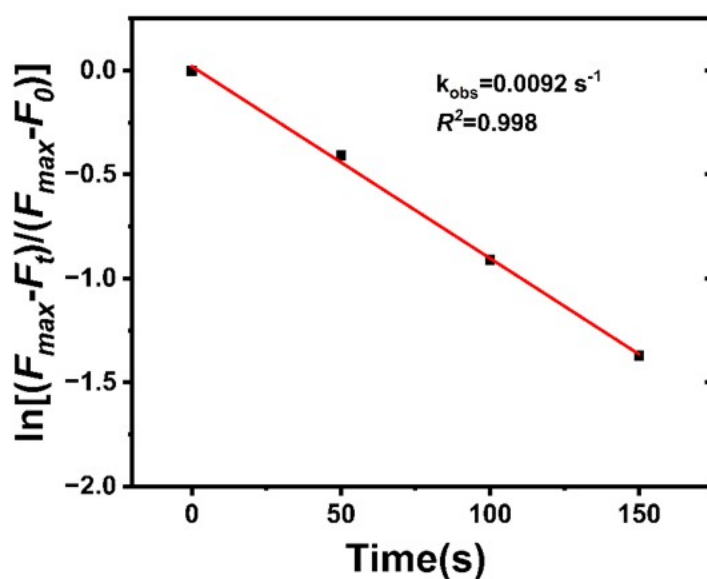


Fig. S10. Pseudo-first-order kinetic plot of the probe DCO-POT (10 μM) with the addition of ONOO⁻ (20 μM) in an MeOH-(Tris-HCl) (1:1 vol%) solution.

8. Cytotoxicity assay

The specific operation of the MTT experiment is as follows: SH-SY5Y cells were seeded in a 96-well microtiter plate and cultured in a 37°C incubator with 5% CO₂ and 95% air for 24 h. Cells were then incubated with probe solutions (0, 5, 10, 15, 20, and 50 μM) at different concentrations for 12 hours, respectively. After incubation, cells were washed three times with PBS. Subsequently, the MTT solution (200 μL , 0.5 mg/mL) was added to each well to continue incubating the cells. After 24 h, the remaining MTT was removed and the formazan crystals were dissolved with DMSO. The absorbance at 570 nm was measured on a microplate reader, and the cell viability was calculated according to the formula: cell viability (%) = (average absorbance of the experimental group/average absorbance of the control group) \times 100%

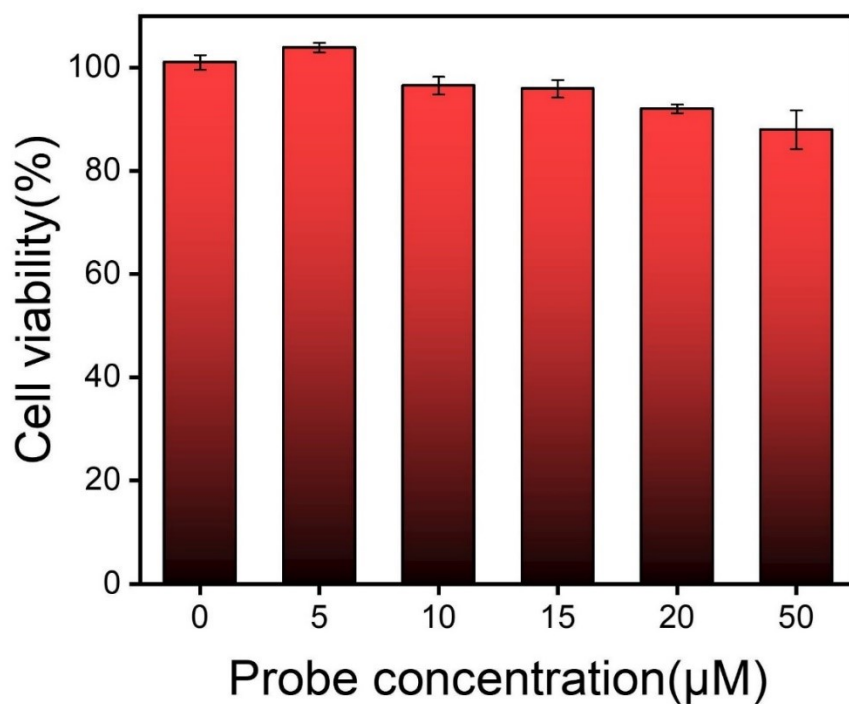
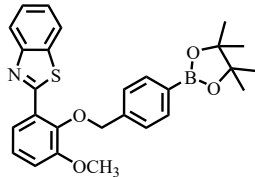
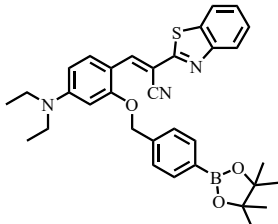
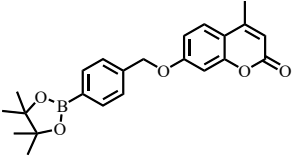
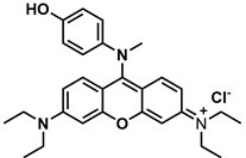
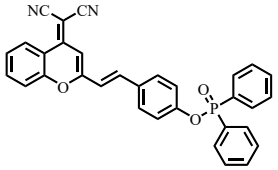
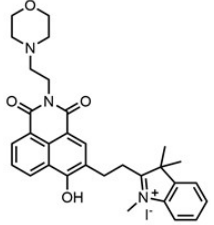
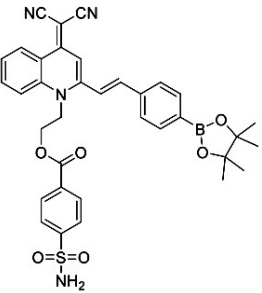
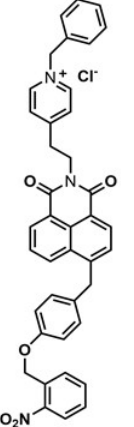
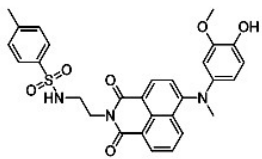


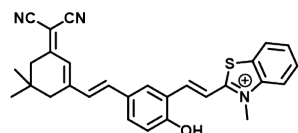
Fig. S11. The cytotoxicity of probe DCO-POT in living SH-SY5Y cells.

9. Comparison of probe DCO-POT with the reported probes

Table S1. Comparison of probe **DCO-POT** with the reported probes for ONOO^- .

Probes	$\lambda_{\text{ex}}/\lambda_{\text{em}}$ (nm)	Detection limit	Subcellular organelle targeting	Ref.
	317/483	26.3 nmol/L	No	[3]
	460/530	15 nmol/L	No	[4]

	322/450	29.8 nmol/L	No	[5]
	440/545	4 nmol/L	Mitochondria	[6]
	556/690	4.62 μmol/L	No	[7]
	440/510	0.24 μmol/L	lysosome	[8]
	420/600	250 nmol/L	Golgi apparatus	[9]
	435/553	48 nmol/L	Mitochondrial	[10]
	488/540	8.3 nmol/L	Endoplasmic reticulum	[11]



500/670

10 nmol/L

Mitochondrial

This work

References:

- [1] W. Shu, S. Zang, C. Wang, M. Gao, J. Jing, X. Zhang, An Endoplasmic Reticulum-Targeted Ratiometric Fluorescent Probe for the Sensing of Hydrogen Sulfide in Living Cells and Zebrafish, *Analytical Chemistry*, 92 (2020) 9982-9988.
- [2] J. Liu, Y.-Q. Sun, Y. Huo, H. Zhang, L. Wang, P. Zhang, D. Song, Y. Shi, W. Guo, Simultaneous Fluorescence Sensing of Cys and GSH from Different Emission Channels, *Journal of the American Chemical Society*, 136 (2014) 574-577.
- [3] Q. Li, Z. Yang, A boronate-based ratiometric fluorescent probe for fast selective detection of peroxynitrite, *Tetrahedron Letters*, 59 (2018) 125-129.
- [4] L. Xia, Y. Tong, L. Li, M. Cui, Y. Gu, P. Wang, A selective fluorescent turn-on probe for imaging peroxynitrite in living cells and drug-damaged liver tissues, *Talanta*, 204 (2019) 431-437.
- [5] S. Palanisamy, P.-Y. Wu, S.-C. Wu, Y.-J. Chen, S.-C. Tzou, C.-H. Wang, C.-Y. Chen, Y.-M. Wang, In vitro and in vivo imaging of peroxynitrite by a ratiometric boronate-based fluorescent probe, *Biosensors and Bioelectronics*, 91 (2017) 849-856.
- [6] H. Zhang, J. Liu, Y.-Q. Sun, Y. Huo, Y. Li, W. Liu, X. Wu, N. Zhu, Y. Shi, W. Guo, A mitochondria-targetable fluorescent probe for peroxynitrite: fast response and high selectivity, *Chemical Communications*, 51 (2015) 2721-2724.
- [7] S.V. Mulay, Y. Kim, K.J. Lee, T. Yudhistira, H.-S. Park, D.G. Churchill, A fluorogenic and red-shifted diphenyl phosphinate-based probe for selective peroxynitrite detection as demonstrated in fixed cells, *New Journal of Chemistry*, 41 (2017) 11934-11940.
- [8] B. Guo, J. Jing, L. Nie, F. Xin, C. Gao, W. Yang, X. Zhang, A lysosome targetable versatile fluorescent probe for imaging viscosity and peroxynitrite with different fluorescence signals in living cells, *Journal of Materials Chemistry B*, 6 (2018) 580-585.
- [9] J. Li, J. Tang, X. Yang, P. Xie, J. Liu, D. Zhang, Y. Ye, A novel aggregation-induced emission fluorescent probe to visualize peroxynitrite levels during Golgi stress, *Sensors and Actuators B: Chemical*, 358 (2022) 131513.
- [10] X. Xie, Y. Liu, G. Liu, Y. Zhao, J. Bian, Y. Li, J. Zhang, X. Wang, B. Tang, Photocontrollable Fluorescence Imaging of Mitochondrial Peroxynitrite during Ferroptosis with High Fidelity, *Analytical Chemistry*, 94 (2022) 10213-10220.
- [11] M. Yan, H. Fang, X. Wang, J. Xu, C. Zhang, L. Xu, L. Li, A two-photon fluorescent probe for visualizing endoplasmic reticulum peroxynitrite in Parkinson's disease models, *Sensors and Actuators B: Chemical*, 328 (2021) 129003.